

Photosubstitution in Tris Chelate Complexes of Ruthenium(II) Containing the Ligands 2,2'-Bipyrazine, 2,2'-Bipyrimidine, 2,2'-Bipyridine, and 4,4'-Dimethyl-2,2'-bipyridine: Energy Gap Control

Helen B. Ross, Massoud Boldaji, D. Paul Rillema,* Charles B. Blanton, and Russell P. White

Received October 12, 1988

Photosubstitution was studied for a series of ruthenium(II) complexes containing the ligands 2,2'-bipyridine (bpy), 2,2'-bipyrimidine (bpm), 2,2'-bipyrazine (bpz), 4,4'-dimethyl-2,2'-bipyridine ((CH₃)₂bpy), pyridine (py), CH₃CN, and Cl⁻. For the study, a number of new complexes were synthesized that include [Ru(bpz)₂(bpm)]²⁺, [Ru((CH₃)₂bpy)₂(py)]²⁺, [Ru(bpm)₂(py)]²⁺, [Ru(bpz)₂(py)]²⁺, [Ru(bpz)(bpy)(py)]²⁺, [Ru(bpm)₂(bpz)]²⁺, [Ru(bpz)(bpm)(bpy)]²⁺, [Ru(bpm)₂(CH₃CN)Cl]⁺, and Ru(bpm)₂Cl₂ and their absorption, emission, and electrochemical properties were determined. The newly synthesized complexes exhibited MLCT transitions that ranged from 439 nm for [Ru((CH₃)₂bpy)₂(py)]²⁺ to 571 nm for Ru(bpm)₂Cl₂, corrected emission maxima that ranged from 615 nm for [Ru((CH₃)₂bpy)₂(py)]²⁺ to 788 nm for [Ru(bpm)₂(CH₃CN)Cl]⁺. Ru(III/II) metal-centered redox potentials that varied from 0.58 V for Ru(bpm)₂Cl₂ to 1.87 V vs SSCE for [Ru(bpz)₂(bpm)]²⁺, ligand-centered reductions, the first of which varied from -0.75 V for [Ru(bpz)₂(bpm)]²⁺ to -1.46 V vs SSCE for [Ru((CH₃)₂bpy)₂(py)]²⁺, and radiative quantum yields that ranged from 0.04 for [Ru(bpz)₂(bpm)]²⁺ to 1.8 × 10⁻⁵ for [Ru(bpm)₂(CH₃CN)Cl]⁺. Photosubstitution quantum yields of the complexes [Ru(bpz)₂(bpm)]²⁺, [Ru(bpm)₂(bpz)]²⁺, [Ru(bpz)(bpm)(bpy)]²⁺, [Ru(bpm)₂(CH₃CN)Cl]⁺, [Ru(bpz)₂(CH₃CN)Cl]⁺, and [Ru(L-L)₂(py)]²⁺ (L-L = (CH₃)₂bpy, bpy, bpm, bpz), and Ru(bpy)_n(L'-L')_{3-n} (n = 0-3; L'-L' = bpz, bpm) were studied in acetonitrile containing 1 mM Cl⁻ at room temperature (25 ± 0.1 °C). The substitution quantum yields ranged from 0.35 for [Ru(bpz)₂]²⁺ to 1.7 × 10⁻⁴ for [Ru(bpy)₂(bpz)]²⁺. The logarithm of the observed photochemical substitution quantum yield was found to correlate linearly with ΔE_{1/2}, where ΔE_{1/2} is the difference in redox potential between the first oxidation and first reduction of the ruthenium complexes. The correlation of ln φ_p(obs) with ΔE_{1/2} occurred in two series: one with complexes containing bpm and bpz ligands and the other with complexes containing only bpy-type ligands. Under a set of limiting conditions, the correlation of ln φ_p(obs) with ΔE_{1/2} was shown to relate to the energy gap law.

Introduction

A number of papers¹⁻¹⁰ on properties of ruthenium polypyridyl complexes have focused on photosubstitution. The results of these studies suggest that the photophysical event involves formation of a five-coordinate intermediate that can either recombine with the original donor atom or add another ligand in the vacant coordination site.⁹ Addition of a negatively charged ligand is favored in solvents where ion pairing occurs between the positively charged ruthenium(II) cation and negatively charged anions. Thus, photosubstitution was enhanced in methylene chloride^{1,3-6} but was considerably less pronounced in water,^{3b,6} particularly without added ligands such as chloride ion.

The photochemical behavior is derived from population of an excited d-d state. Henderson and Cherry⁶ concluded that the ligand field state was short-lived and rapidly dissociated into the five-coordinate intermediate or underwent radiationless decay. Kalyanasundaram⁷ noted that bipyrazine ligand loss in [Ru-(bpz)₃]²⁺ occurred on a time scale comparable to that of the decay of the ³MLCT state. For tris chelate complexes, the d-d state is thought to be populated directly from the ³MLCT state.¹¹

However, for complexes of the type [Ru(bpy)₂XY]ⁿ⁺, where bpy is 2,2'-bipyridine and X and Y are monodentate ligands, recent evidence suggests that the d-d state may be populated by a higher lying singlet state.^{5,6} A potential energy surface diagram used to summarize photophysical features related to ruthenium(II) heterocycles is shown in Figure 1.

The presence of the low-lying d-d state is a nuisance in attempts to design new photocatalysts, and steps are being explored to minimize its effect. In mixed-chelates [Ru(L-L)_{3-n}(bpy)_n]²⁺ (n = 1,2; L-L = 2,2'-bipyrazine, 2,2'-bipyrimidine, 2,3-bis(2-pyridyl)quinoxaline, 2,2'-biisoquinoline)^{8,12} ligand loss was quenched for the complexes [Ru(L-L)(bpy)₂]²⁺. The reasons for this may be related to the relative energy position of the d-d state compared to that of the ³MLCT state. The combination of the low-lying π* level localized on L-L in [Ru(L-L)(bpy)₂]²⁺ and the average ligand field strength may result in greater spacing between two energy levels and, thereby, decrease ligand loss.^{11,12}

In the study reported here, we have investigated the role played by the lowest lying π* energy level localized on L-L in directing photosubstitution in mixed-ligand ruthenium(II) heterocycles and have examined this in terms of the photophysical properties,⁸ particularly as the photochemical substitution quantum yield is related to nonradiative decay rate constants. The complexes that we have studied are ruthenium(II) heterocycles containing various combinations of ligands illustrated in Figure 2. The results of the study lead to a clearer understanding of the photophysical events responsible for the observed photochemistry.

Experimental Section

Materials. RuCl₃·3H₂O was a gift from Johnson-Matthey, Inc. The ligands 2,2'-bipyridine, 4,4'-dimethyl-2,2'-bipyridine, and 2,2'-bipyrimidine were purchased commercially and used without further purification. Acetonitrile was of HPLC grade and was dried over 4-Å molecular sieves before use. Electrolytes, tetraethylammonium perchlorate (TEAP), tetraethylammonium hexafluorophosphate (TEAH), and tetrabutylammonium hexafluorophosphate (TBAH), were Electrograde from Southwestern Analytical. The salts were dried in a vacuum oven at 70 °C overnight before use. Tetraethylammonium chloride ((TEA)Cl), purchased from Aldrich, was purified by using the procedure

- (1) (a) Gleria, M.; Minto, F.; Beggato, G.; Bortolus, P. *J. Chem. Soc., Chem. Commun.* **1978**, 285. (b) Jones, R. F.; Cole-Hamilton, D. J. *Inorg. Chim. Acta* **1981**, 53, L3. (c) Fetterolf, M. L.; Offen, H. W. *Inorg. Chem.* **1987**, 26, 1070.
- (2) (a) Hoggard, P. E.; Porter, G. B. *J. Am. Chem. Soc.* **1978**, 100, 1457. (b) Wallace, W. M.; Hoggard, P. E. *Inorg. Chem.* **1980**, 19, 2141. (c) Fasano, R.; Hoggard, P. E. *Ibid.* **1983**, 22, 566.
- (3) (a) Durham, B.; Walsh, J. L.; Carter, C. L.; Meyer, T. J. *Inorg. Chem.* **1980**, 19, 850. (b) Durham, B.; Caspar, J. V.; Nagle, J. K.; Meyer, T. J. *J. Am. Chem. Soc.* **1982**, 104, 4803.
- (4) (a) Wacholtz, W. M.; Auerbach, R. A.; Schmehl, R. H.; Ollino, M.; Cherry, W. R. *Inorg. Chem.* **1985**, 24, 1758. (b) Wacholtz, W. F.; Auerbach, R. A.; Schmehl, R. H. *Ibid.* **1986**, 25, 227.
- (5) (a) Pinnick, D. V.; Durham, B. *Inorg. Chem.* **1984**, 23, 1440. (b) Pinnick, D. V.; Durham, B. *Ibid.* **1984**, 23, 3841.
- (6) Henderson, L. J.; Cherry, W. R. *Chem. Phys. Lett.* **1985**, 114, 553.
- (7) Kalyanasundaram, K. *J. Phys. Chem.* **1986**, 90, 2285.
- (8) (a) Allen, G. H.; White, R. P.; Rillema, D. P.; Meyer, T. J. *J. Am. Chem. Soc.* **1984**, 106, 2613. (b) Rillema, D. P.; Taghdiri, D. G.; Jones, D. S.; Keller, C. D.; Worl, L. A.; Meyer, T. J.; Levy, H. A. *Inorg. Chem.* **1987**, 26, 578.
- (9) (a) VanHouten, J.; Watts, R. J. *Inorg. Chem.* **1978**, 17, 3381. (b) Watts, R. J. *J. Chem. Educ.* **1983**, 60, 834.
- (10) Kirchhoff, J. R.; McMillin, D. R.; Marnot, P. A.; Sauvage, J. P. *J. Am. Chem. Soc.* **1985**, 107, 1138.

(11) Meyer, T. J. *Pure Appl. Chem.* **1986**, 58, 1193.

(12) Barigelletti, F.; Juris, A.; Balzani, V.; Belser, P. *Inorg. Chem.* **1983**, 22, 3335.

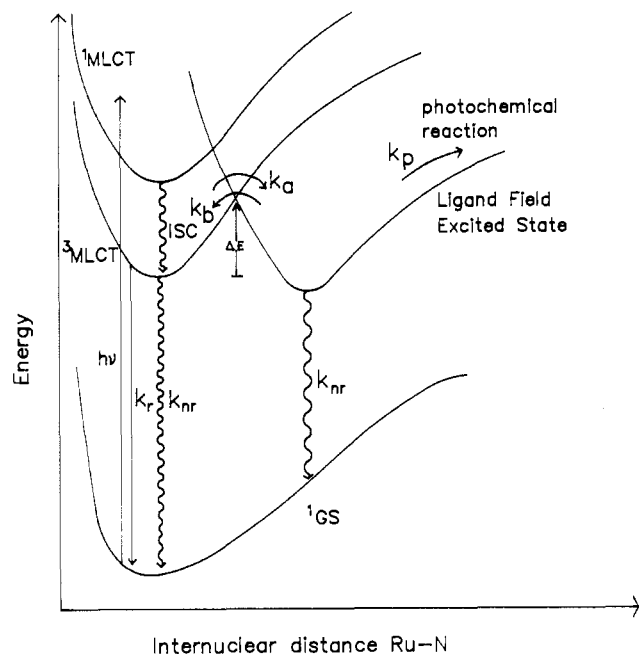


Figure 1. Potential energy surfaces relating excited-state photophysical events to photosubstitution.

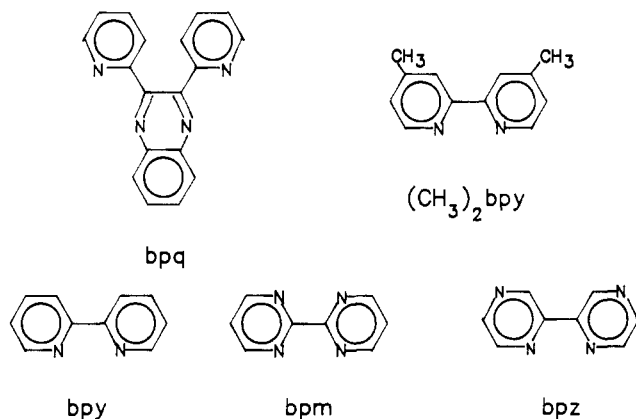


Figure 2. Heterocyclic ligands employed in this report. The ligand bpy is 2,2'-bipyridine, bpm is 2,2'-bipyrimidine, bpz is 2,2'-bipyrazine, $(\text{CH}_3)_2\text{bpy}$ is 4,4'-dimethyl-2,2'-bipyridine, and bpq is 2,3-bis(2-pyridyl)quinoxaline.

of Unni, Elias, and Schiff.¹³ The crystals were dried and stored in a vacuum desiccator. All other reagents were purchased as reagent grade and used without further purification.

Preparation of Compounds. $[\text{Ru}(\text{bpz})_3](\text{PF}_6)_2$, $[\text{Ru}(\text{bpz})_2(\text{bpy})](\text{PF}_6)_2$, $[\text{Ru}(\text{bpz})_2(\text{bpy})](\text{PF}_6)_2$, $[\text{Ru}(\text{bpm})_3](\text{PF}_6)_2$, and $[\text{Ru}(\text{bpm})_2(\text{bpy})](\text{PF}_6)_2$ were prepared as previously described.^{14a} $\text{Ru}(\text{bpy})_2\text{Cl}_2$, $\text{Ru}(\text{bpy})\text{Cl}_4$, and $[\text{Ru}(\text{bpy})_3]\text{Cl}_2$ were available in our laboratories from previous studies. Elemental analyses of new compounds were carried out by Atlantic Microlabs, Inc., Norcross, GA. These accompany the paper as supplementary material (Table IV).

$[\text{Ru}(\text{bpy})_2((\text{CH}_3)_2\text{bpy})](\text{PF}_6)_2$. $[\text{Ru}(\text{bpy})_2((\text{CH}_3)_2\text{bpy})](\text{PF}_6)_2$ was prepared by using a modification of the procedure developed by Valenty, Behnken, and Gaines.^{14b} $\text{Ru}(\text{bpy})_2\text{Cl}_2$ (0.20 g, 0.38 mmol) and 4,4'-dimethyl-2,2'-bipyridine (0.30 g, 1.62 mmol) were added to a 25-mL flask containing 8 mL of ethylene glycol. The suspension was heated to reflux for 1 h, during which time the solution color changed from dark green to orange. The solution was cooled to room temperature and diluted with 8 mL of H_2O , and the resultant mixture was filtered to remove excess ligand. Saturated, aqueous NH_4PF_6 was added dropwise to the filtrate until precipitation was complete. The solid material was then removed by filtration, redissolved in acetonitrile, and reprecipitated by addition to swirling ether. The compound was purified by column chromatogra-

phy as outlined previously.^{8b} (Yield = 94%.)

$[\text{Ru}((\text{CH}_3)_2\text{bpy})_2(\text{bpy})](\text{PF}_6)_2$. The same procedure as outlined above for the preparation of $[\text{Ru}(\text{bpy})_2((\text{CH}_3)_2\text{bpy})](\text{PF}_6)_2$ was used except that 0.20 g (0.46 mmol) of $\text{Ru}(\text{bpy})\text{Cl}_4$ and 0.26 g (1.39 mmol) of 4,4'-dimethyl-2,2'-bipyridine were used. (Yield = 95%.)

$[\text{Ru}(\text{bpz})_2(\text{CH}_3\text{CN})\text{Cl}](\text{PF}_6)$. $[\text{Ru}(\text{bpz})_2(\text{CH}_3\text{CN})\text{Cl}](\text{PF}_6)$ was prepared by using a modification of the procedure developed by Crutchley and Lever.¹⁵ A 0.75-g quantity of $[\text{Ru}(\text{bpz})_3](\text{PF}_6)_2$ (8.7×10^{-4} mol) was dissolved in 1000 mL of acetonitrile. This solution was stirred and irradiated in a Pyrex cylinder for 5 min. The irradiations were effected at 3500 Å with a Rayonet photochemical reactor. (TEA)Cl, 5% in excess of a 1:1 molar ratio, was dissolved in 100 mL of acetonitrile, and the solution was slowly added to the irradiating solution over a 25-min interval. The photolysis flask was covered while the photoreaction proceeded. The temperature of the solution in the photoreactor was $\sim 40^\circ\text{C}$. Samples were taken from the reaction mixture during the photolysis, and luminescence spectra were obtained. As the reaction proceeded, the emission peak due to $[\text{Ru}(\text{bpz})_3]^{2+}$ at 610 nm decreased in intensity. Since concentration was approximately proportional to luminescence intensity, the luminescence intensities were used to determine when most of the $[\text{Ru}(\text{bpz})_3]^{2+}$ had reacted. The reaction was stopped when the 610-nm peak was reduced to a shoulder on the uncorrected emission peak at 725 nm. This normally took approximately 8 h.

After the reaction had proceeded to a point where the 610-nm luminescence peak was reduced to a shoulder on the emission peak at 725 nm, the reaction mixture was evaporated to dryness on a rotary evaporator and washed with 1-propanol and then ether. The solid was dissolved in acetone and precipitated by removing solvent on the rotary evaporator. Unreacted $[\text{Ru}(\text{bpz})_3]^{2+}$ remained in solution, while the product, which was less soluble in acetonitrile, precipitated. The solid from the precipitation was dissolved in acetonitrile, and the solution was divided into three equal portions. Each portion was chromatographed once on a Sephadex LH-60 column using acetonitrile as the solvent and the eluent. The columns were $3/4$ in. wide and 8 in. long. Small samples were taken from each fraction of the column and mixed with 0.1 M TEAP in acetonitrile. Cyclic voltammograms were obtained on these samples to determine their purity. There were two components: the first was $[\text{Ru}(\text{bpz})_2(\text{CH}_3\text{CN})\text{Cl}]^+$; the second, $[\text{Ru}(\text{bpz})_2\text{Cl}_2]$. A very slow drip rate (one drop/13 s) was necessary to separate the two components. The purest $[\text{Ru}(\text{bpz})_2(\text{CH}_3\text{CN})\text{Cl}]^+$ fractions of the column were collected. These fractions were filtered and reduced by evaporation on the rotary evaporator until the volume was 10–15 mL. $[\text{Ru}(\text{bpz})_2(\text{CH}_3\text{CN})\text{Cl}](\text{PF}_6)$ was precipitated from this solution by addition to swirling ether. (Yield = 0.09 g, 67%.)

$[\text{Ru}(\text{bpm})_2(\text{CH}_3\text{CN})\text{Cl}](\text{PF}_6)$. The procedure to make this compound was similar to the one used to make $[\text{Ru}(\text{bpz})_2(\text{CH}_3\text{CN})\text{Cl}](\text{PF}_6)$. A 0.50-g quantity of $[\text{Ru}(\text{bpm})_3](\text{PF}_6)_2$ (5.8×10^{-4} mol) was dissolved in 1000 mL of acetonitrile, and the solution was stirred and irradiated for 5 min. A solution of 0.1 g (6.1×10^{-4} mol) of (TEA)Cl in 100 mL of acetonitrile was added slowly over 15 min to the irradiating solution. This mixture was photolyzed for 24 h. The reaction mixture was evaporated to dryness, and the solid was washed with cold 1-propanol and then ether. The product was dissolved in a minimum amount of acetonitrile and divided into two portions. Each portion was chromatographed once on neutral alumina columns $3/4$ in. in diameter and 4 in. long. Small samples were taken from the eluate and mixed with 0.1 M TEAP in acetonitrile. Cyclic voltammograms and luminescence spectra were then obtained to identify the components of the fractions from the columns. The first component was $[\text{Ru}(\text{bpm})_2(\text{CH}_3\text{CN})\text{Cl}]^+$, and the second was unreacted $[\text{Ru}(\text{bpm})_3]^{2+}$. A third component did not elute. The alumina containing this component was removed from the column and washed with methanol, and the resultant mixture was then filtered. The volume of the filtrate was reduced to dryness by evaporation of the solvent on the rotary evaporator. Then the dry residue was dissolved in 0.1 M TEAP in acetonitrile, and the third fraction was identified by cyclic voltammetry as $\text{Ru}(\text{bpm})_2\text{Cl}_2$. The fractions containing the purest $[\text{Ru}(\text{bpm})_2(\text{CH}_3\text{CN})\text{Cl}]^+$ were collected. A slow (one drop/s) drip rate was necessary to separate the desired material from the unreacted starting material and other components that were directly above it. The purest eluate was concentrated to 30 mL, and $[\text{Ru}(\text{bpm})_2(\text{CH}_3\text{CN})\text{Cl}](\text{PF}_6)$ was precipitated from this solution by addition to swirling ether. (Yield = 0.20 g, 55%.)

$[\text{Ru}(\text{bpz})_2\text{Cl}_2]$. This procedure is a modification of the one used by Crutchley and Lever.¹⁵ A 0.151-g quantity of $[\text{Ru}(\text{bpz})_2(\text{CH}_3\text{CN})\text{Cl}](\text{PF}_6)$ (2.4×10^{-4} mol) was dissolved in 1000 mL of acetonitrile. The solution was stirred and irradiated at 3500 Å. To this solution was slowly added 2.4 g of (TEA)Cl (1.4×10^{-2} mol) in 100 mL of acetonitrile over

(13) Unni, A. K. R.; Elias, L.; Schiff, H. I. *J. Phys. Chem.* **1963**, *67*, 1216.
(14) (a) Rillema, D. P.; Allen, G.; Meyer, T. J.; Conrad, D. *Inorg. Chem.* **1983**, *22*, 1617. (b) Valenty, S. J.; Behnken, D. E.; Gaines, G. L., Jr. *Inorg. Chem.* **1979**, *18*, 2160.

(15) Crutchley, R. J.; Lever, A. P. B. *Inorg. Chem.* **1982**, *21*, 2276.

a 15-min interval. The solution was stirred and irradiated for 23 h. The reaction mixture was filtered and the filtrate reduced in volume to dryness by removal of the solvent on the rotary evaporator. This solid was dissolved in 1-propanol and then precipitated from solution by the addition of ether. (Too much ether caused the formation of a white solid.) $\text{Ru}(\text{bpz})_2\text{Cl}_2$ was filtered off and washed on the frit with ether and then acetonitrile. Small amounts of the solid were mixed with 0.1 M TEAP in acetonitrile, and a cyclic voltammogram and luminescence spectrum were obtained. The cyclic voltammogram showed only one component with the appropriate $E_{1/2}$ value, and no luminescence was observed at room temperature. (Yield = 0.095 g, 82%.)

[Ru(bpm)₂Cl₂]. A procedure similar to the one directly above was followed except that 0.301 g of $[\text{Ru}(\text{bpm})_2(\text{CH}_3\text{CN})\text{Cl}](\text{PF}_6)$ (4.7×10^{-4} mol) and 0.84 g of $(\text{TEA})\text{Cl}$ (5.1×10^{-3} mol) were used. After the volume of the irradiated solution was reduced to dryness by removal of the solvent on the rotary evaporator, the solid was washed in 1-propanol and then ether. It was then washed with acetonitrile until the liquid turned from scarlet to light bluish purple. (The reactant, $[\text{Ru}(\text{bpm})_2(\text{CH}_3\text{CN})\text{Cl}](\text{PF}_6)$, is soluble in acetonitrile and gave a scarlet solution.) Solid $\text{Ru}(\text{bpm})_2\text{Cl}_2$ remained on the filter frit. (Yield = 0.060 g, 26%.)

[Ru(bpz)₂(bpm)](PF₆)₂. Method A. A 0.15-g quantity of $[\text{Ru}(\text{bpz})_2(\text{CH}_3\text{CN})\text{Cl}](\text{PF}_6)$ (2.3×10^{-4} mol) and 0.11 g of 2,2'-bipyrimidine (6.9×10^{-4} mol) were suspended in 30 mL of ethylene glycol. The solution was heated gradually. As it began to reflux, a red precipitate formed. The solution was cooled, but it was not filtered. A minimum amount of saturated aqueous NH_4PF_6 was added to the reaction mixture to precipitate the rest of the product from the ethylene glycol. The solid PF_6^- salt was washed with ether and then dissolved in a minimum amount of acetonitrile. The solution was chromatographed on a neutral alumina column using acetonitrile as the solvent and eluent. The column was $3/4$ in. in diameter and four in. long. There were three components. The major fraction, which was orange and contained the product, was the first to elute. Two other components were brown and were located above the main fraction on the column. Small samples were taken from the main eluate and mixed with 0.1 M TEAP. Cyclic voltammograms of these samples were obtained in order to determine which fractions were the purest. The purest fractions of the main component (the product) were combined and filtered. The volume of these fractions was reduced to 10–15 mL by evaporation of the solvent using a rotary evaporator. The product was precipitated by addition of this solution to swirling ether.

Method B. $\text{Ru}(\text{bpz})_2\text{Cl}_2$ (0.15 g) and 0.056 g of 2,2'-bipyrimidine were suspended in 10 mL of ethylene glycol, and the mixture was heated at reflux for 10 min. The solution was cooled to room temperature, and excess ligand was removed by filtration. The cation was precipitated as the hexafluorophosphate salt, effected by the addition of a saturated aqueous NH_4PF_6 solution until precipitation ceased. The product was collected by filtration and purified by passing a concentrated acetonitrile solution of the crude product over a neutral alumina column.

[Ru(bpm)₂(bpz)](PF₆)₂. $\text{Ru}(\text{bpm})_2\text{Cl}_2$ (0.18 g) and a 2-fold excess of 2,2'-bipyrazine were suspended in 10 mL of ethylene glycol, and the mixture was heated at reflux for 30 min. The solution was cooled to room temperature and filtered to remove excess ligand. The cation was isolated as the hexafluorophosphate salt by addition of a saturated aqueous NH_4PF_6 solution until precipitation was complete. The salt was isolated, washed with ether, and redissolved in a small amount of acetonitrile. The solution was then chromatographed on neutral alumina, and the fractions were monitored by cyclic voltammetry as outlined above. The purest fractions were then combined, the volume was reduced to about 10 mL by rotary evaporation, and the complex was isolated by addition of the concentrate to swirling ether.

[Ru(bpz)(bpm)(bpy)](PF₆)₂. $[\text{Ru}(\text{bpm})_2(\text{CH}_3\text{CN})\text{Cl}](\text{PF}_6)$ (0.64 g) and a 2-fold excess of 2,2'-bipyridine were suspended in 25 mL of ethylene glycol, and then the mixture was heated at reflux for 30 min. The solution was cooled, and excess ligand was removed by filtration. The $[\text{Ru}(\text{bpm})_2(\text{bpy})]^{2+}$ cation was isolated as the PF_6^- salt as outlined above and purified by column chromatography as described previously.¹⁴ A 0.17-g sample of $[\text{Ru}(\text{bpm})_2(\text{bpy})](\text{PF}_6)_2$ was then dissolved in a 1000-mL solution of acetonitrile containing 0.10 g of tetraethylammonium chloride, and the solution was irradiated in a Pyrex cylinder. The irradiation was effected at 3500 Å with a Rayonet photochemical reactor and carried out for ~24 h. The resulting solution containing $[\text{Ru}(\text{bpm})(\text{bpy})(\text{CH}_3\text{CN})\text{Cl}]^+$ was concentrated to ~20 mL, and then a saturated aqueous NH_4PF_6 solution was added to precipitate the complex cation as the PF_6^- salt. It was isolated, washed with ether, and dissolved in a minimum amount of acetonitrile. The solution was then chromatographed as outlined previously for acetonitrile chloro derivatives, and the product was isolated by procedures outlined above. Then a 0.070-g sample of $[\text{Ru}(\text{bpm})(\text{bpy})(\text{CH}_3\text{CN})\text{Cl}](\text{PF}_6)$ and 0.47 g of 2,2'-bipyrazine were suspended in 10 mL of ethylene glycol, and the

mixture was refluxed until the color of the solution changed from red to orange. The procedures used above to isolate and purify mixed-ligand complexes were followed to obtain $[\text{Ru}(\text{bpz})(\text{bpm})(\text{bpy})](\text{PF}_6)_2$.

[Ru(bpm)₃]Cl₂. Commercial $\text{RuCl}_3 \cdot 3\text{H}_2\text{O}$ (0.60 g, 2.3 mmol) and 2,2'-bipyrimidine (1.81 g, 11.5 mmol) were heated at reflux and stirred in 40 mL of ethylene glycol for 1 h. After cooling, the solution was filtered to remove excess bipyrimidine. The filtrate was placed in the freezer overnight, during which time a red precipitate formed (pure $[\text{Ru}(\text{bpm})_3]\text{Cl}_2$). The solution was filtered and the precipitate air-dried.

A second crop was obtained upon addition of the filtrate to acetone. The product was collected by filtration and purified by column chromatography as outlined previously.^{8b}

[Ru(bpz)₃]Cl₂. A similar procedure as outlined above for the preparation of $[\text{Ru}(\text{bpm})_3]\text{Cl}_2$ was used for the preparation of $[\text{Ru}(\text{bpz})_3]\text{Cl}_2$. In this case, 0.292 g (1.85 mmol) of $\text{RuCl}_3 \cdot 3\text{H}_2\text{O}$ and 1.02 g (6.44 mmol) of 2,2'-bipyrazine were the source materials, and after reflux in ethylene glycol, the product was isolated by addition of the reactant solution to acetone.

[Ru(bpy)₃](CF₃SO₃)₂, [Ru((CH₃)₂bpy)₃](CF₃SO₃)₂, [Ru(bpm)₃](CF₃SO₃)₂, and [Ru(bpz)₃](CF₃SO₃)₂. These complexes were prepared by metathesis from the chloride salts. A stoichiometric quantity of $\text{Ag}(\text{CF}_3\text{SO}_3)$ was mixed with the appropriate complex in water. AgCl was removed by filtration, and the filtrate was concentrated on a hot plate until the product precipitated. The resulting orange crystals were filtered, washed with a small amount of distilled water, and air-dried.

[Ru(bpy)₂(py)₂](CF₃SO₃)₂, [Ru(bpz)₂(py)₂](CF₃SO₃)₂, and [Ru((CH₃)₂bpy)₂(py)₂](CF₃SO₃)₂. Each $[\text{Ru}(\text{L}-\text{L})_3](\text{CF}_3\text{SO}_3)_2$ complex, where $\text{L}-\text{L} = \text{bpy}$, $(\text{CH}_3)_2\text{bpy}$, or bpz , was added to neat trifluoromethanesulfonic acid, HTRIF, and the resulting solution was refluxed under nitrogen for 1 h. After cooling, the solution was slowly added to anhydrous ethyl ether. The resulting precipitate was collected under nitrogen by Schlenk-ware techniques. The product was then added to neat pyridine, and the mixture was refluxed for 1 h. After cooling to room temperature, the solution was added to an excess of swirling ether. The resulting precipitate was collected by filtration, washed with ether, and dried under vacuum. The product was purified by column chromatography as outlined previously.^{8b}

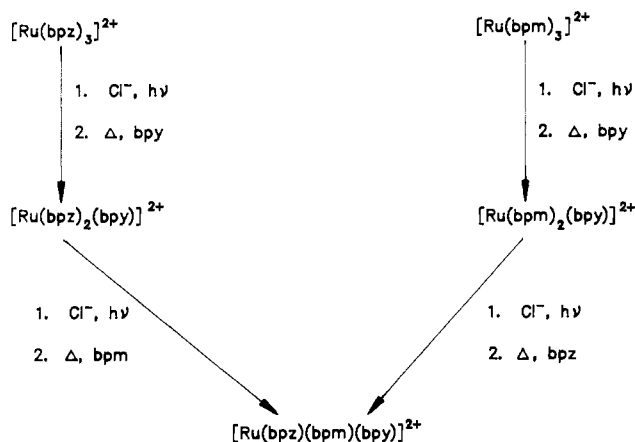
A typical preparation involved the use of 0.10 g of $[\text{Ru}(\text{L}-\text{L})_3](\text{CF}_3\text{SO}_3)_2$ in 2 mL of HTRIF followed by addition of the reactant solution to 100 mL of ether. The resulting product, which analyzed for $[\text{Ru}(\text{L}-\text{L})_2(\text{TRIF})_2]\text{TRIF} \cdot x\text{HTRIF}$, was then added to neat pyridine. In this case, ~0.20 g of complex was added to 30 mL of pyridine, and the mixture, after reflux, was added to ~250 mL of ether to precipitate the product. It was then isolated as described above.

[Ru(bpz)(bpy)(CH₃CN)Cl](PF₆)₂. $[\text{Ru}(\text{bpz})_2(\text{bpy})](\text{PF}_6)_2$ (0.50 g, 0.58 mmol) was dissolved in 900 mL of acetonitrile. The solution was irradiated at 3500 Å with a Rayonet photochemical reactor and was magnetically stirred during the irradiation. A solution of tetraethylammonium chloride ($(\text{TEA})\text{Cl}$) (0.10 g, 0.61 mmol) in 100 mL of acetonitrile was slowly added to the solution under irradiation over a period of 40 min. The resulting solution was photolyzed for 48 h. The solution was then evaporated to dryness, and the resulting precipitate was washed with cold 1-propanol and dry ether. The product was purified by chromatography as described for the preparation of $[\text{Ru}(\text{bpm})_2(\text{CH}_3\text{CN})\text{Cl}](\text{PF}_6)_2$.

[Ru(bpm)₂(py)₂](CF₃SO₃)₂ and [Ru(bpz)(bpy)(py)₂](CF₃SO₃)₂. The procedure was similar to the preparation of $[\text{Ru}(\text{bpy})_2(\text{py})_2](\text{CF}_3\text{SO}_3)_2$. In this case, however, $[\text{Ru}(\text{bpm})_2(\text{CH}_3\text{CN})\text{Cl}]\text{PF}_6$ and $[\text{Ru}(\text{bpz})(\text{bpy})(\text{CH}_3\text{CN})\text{Cl}]\text{PF}_6$ were the starting materials. The compounds were refluxed in neat HTRIF, resulting in displacement of CH_3CN and Cl to give $[\text{Ru}(\text{bpm})_2(\text{TRIF})_2]\text{TRIF} \cdot x\text{HTRIF}$ and $[\text{Ru}(\text{bpz})(\text{bpy})(\text{TRIF})_2]\text{TRIF} \cdot x\text{HTRIF}$. These were isolated by addition of the HTRIF solution to ether. The product was then added to neat pyridine, and the mixture was refluxed for 1 h. The bis(pyridine) complexes were then isolated as described for the preparation of $[\text{Ru}(\text{bpy})_2(\text{py})_2](\text{CF}_3\text{SO}_3)_2$.

Physical Measurements. Cyclic voltammetry measurements were performed in acetonitrile at a platinum-disk working electrode with 0.10 M TEAP, 0.10 M TBAH, or 0.10 M TEAH as the supporting electrolyte. The measurements were made vs the saturated sodium calomel electrode (SSCE). The measurements were made with a PAR 173 potentiostat in conjunction with a PAR 175 universal programmer or a PAR 174A polarographic analyzer modified with a supercycle for voltage control. The cyclic voltammograms were plotted on an IBM 742 MT X-Y-T recorder.

Visible-UV spectra were determined with a Cary 14 spectrophotometer or a Perkin-Elmer Lambda Array 3840 UV/vis spectrophotometer in the high-resolution mode. Beer's law studies were carried out for absorption coefficient determinations at absorption maxima. At least five points were fitted to a linear least-squares program with resulting correlation coefficients of 0.999 and intercepts near zero.

Scheme I. Synthetic Guide for the Synthesis of Several Acetonitrile Chloro, Dichloro, and Mixed-Ligand Ruthenium(II) Complexes

Corrected emission spectra were determined with a Spex F2121 spectrofluorometer or an SLM Instruments, Inc., Model 800 photon-counting fluorescence instrument. Uncorrected emission spectra and emission changes were determined with a Hitachi Perkin-Elmer 650-40 luminescence spectrophotometer. Emission quantum yields were determined in N_2 -degassed acetonitrile solutions at 25 °C by the relative method using $[\text{Ru}(\text{bpy})_3]^{2+}$ as the standard,¹⁶ and calculations were carried out as described previously.^{8b} Luminescence lifetimes were determined in N_2 -degassed acetonitrile solutions at room temperature by using a Molecron UV-400 nitrogen laser as a pulsed light source. The complete lifetime determining system was described earlier.^{14a}

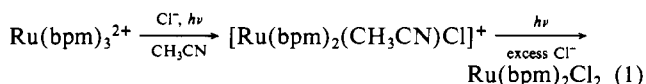
Photochemical quantum yields were measured for a series of ruthenium(II) heterocycles in N_2 -degassed acetonitrile solutions containing 1 mM (TEA)Cl. The procedure used was a modification of an earlier one where precipitation of several ruthenium(II) complexes may have gone undetected during photosubstitution quantum yield determinations in 2 mM (TEA)Cl solutions.^{8a} A Schoeffel system consisting of a 1000-W xenon lamp in an LH 151 N lamp housing, a Model LPS 255 HR universal arc lamp power supply, a GM 252 dual-grating monochromator, and a thermostated cell holder mounted on an optical rail were used for most of the photolysis investigations. For other steady-state photolyses, an apparatus consisting of a PTI LPS200X 150-W photolysis system, an Oriel Model 77250 monochromator, and as cell holder mounted on an optical rail was used. Temperature control was effected with a Haake FK-2 constant-temperature bath, and stirring was effected with TRI-R microsubmersible stirrers. The light intensity was determined at 436 nm with Reinecke's salt,¹⁷ taking care to correct for light transmitted from the cell. The light intensity of the Schoeffel source was 2.88×10^{-9} einstein/s; that of the PTI source was 8.35×10^{-9} einstein/s. The photolysis of the sample was allowed to proceed to a maximum of 10% conversion to product. The extent of photolysis was determined by loss of emission intensity at the emission energy maximum of the parent compound. Preparations of sample solutions for photolysis followed literature procedures.^{3b} The absorbances usually ranged between 0.2 and 0.5 at 436 nm.

Computations were carried out with an IBM PC/XT microcomputer. The data were analyzed by a statistical, nonlinear least-squares program called FLEXFIT.¹⁸

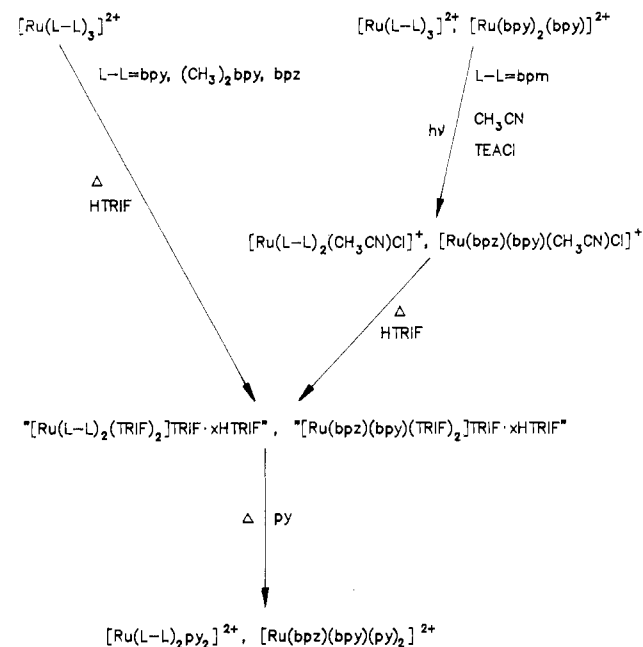
Proton NMR spectra were obtained with a QE300 General Electric FTNMR spectrometer. Deuterated acetonitrile was the solvent.

Results

Preparation of Compounds. Most of the ruthenium complexes reported here were synthesized according to Schemes I and II. The preparative procedures employed both thermal and photochemical methodology. The photochemical procedures followed those of Crutchley and Lever¹⁵ and are illustrated in eq 1.

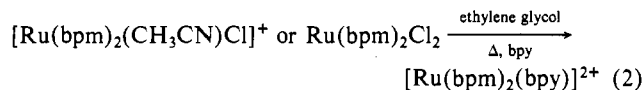


Photolysis of acetonitrile solutions containing the tris chelates and

Scheme II. Synthetic Guide for the Synthesis of Ruthenium(II) Bis(pyridine) Complexes from Tris Chelate Precursors

low concentrations of Cl^- resulted in formation of the acetonitrile complexes. Solutions that contained high concentrations of Cl^- , however, formed the dichloro species via secondary photolysis.

In contrast to the chloride ligands of $\text{Ru}(\text{bpy})_2\text{Cl}_2$, those from analogous bpz or bpm complexes and their acetonitrile chloro analogues were difficult to remove with Ag^+ . Consequently, the preparation of mixed-ligand heterocycles was effected by thermal displacement of the Cl^- ligands in refluxing ethylene glycol. The presence of the appropriate bidentate ligand resulted in formation of the desired complex as illustrated in eq 2.



In Scheme I, the bipyridine ligand was added to $[\text{Ru}(\text{bpz})_2(\text{CH}_3\text{CN})\text{Cl}]^+$ and $[\text{Ru}(\text{bpm})_2(\text{CH}_3\text{CN})\text{Cl}]^+$ to form $[\text{Ru}(\text{bpz})_2(\text{bpy})]^{2+}$ and $[\text{Ru}(\text{bpm})_2(\text{bpy})]^{2+}$, respectively, as an intermediate step in the preparation of $[\text{Ru}(\text{bpz})(\text{bpm})(\text{bpy})]^{2+}$. Photolysis of $[\text{Ru}(\text{bpz})_2(\text{bpy})]^{2+}$ and $[\text{Ru}(\text{bpm})_2(\text{bpy})]^{2+}$ resulted in loss of the bidentate ligand with the lowest π^* energy level. The ligand lost can readily be ascertained from the values of the free-ligand reduction potentials, which are -1.76 V for bpz,¹⁵ -1.80 V for bpm,¹⁹ and -2.21 V for bpy.²⁰ The products from the photolysis step, $[\text{Ru}(\text{bpz})(\text{bpy})(\text{CH}_3\text{CN})\text{Cl}]^+$ and $[\text{Ru}(\text{bpm})(\text{bpy})(\text{CH}_3\text{CN})\text{Cl}]^+$, were then complexed with bpm and bpz, respectively, to give the final product illustrated in the scheme. In mixed-ligand complexes containing bidentate chelating ligands, it is clear from the synthetic evidence that the lowest energy ³MLCT state resides on the ligand with the lowest π^* energy level and it is the one lost upon photolysis. This can be explained by the localized-orbital model, which places the excited-state electron density on one of the heterocyclic ligands^{21,22} rather than all three.

Similar procedures were used to prepare $[\text{Ru}(\text{bpm})_2(\text{bpz})]^{2+}$ and $[\text{Ru}(\text{bpz})_2(\text{bpm})]^{2+}$. The parent tris chelates were photolyzed in acetonitrile containing Cl^- . The acetonitrile chloro complexes along with the appropriate ligand were used to effect preparation of the desired products.

(19) Measured by K. Goldsky, The University of North Carolina at Chapel Hill, in 0.1 M TEAP-acetonitrile solution at an Ag reference electrode. The reduction was irreversible.

(20) Weiner, M. A.; Basu, A. *Inorg. Chem.* **1980**, *19*, 2797.

(21) Brateman, P. S.; Heath, G. A.; Yellowless, L. J. *J. Chem. Soc., Dalton Trans.* **1985**, 1081.

(22) DeArmond, M. K.; Hanck, K. H.; Wertz, D. *Coord. Chem. Rev.* **1985**, *64*, 65.

(16) Kober, E. M.; Meyer, T. J. *Inorg. Chem.* **1982**, *21*, 3967.

(17) Wegner, E. E.; Adamson, A. W. *J. Am. Chem. Soc.* **1966**, *88*, 394.

(18) Ramette, R. W. "FLEXFIT"; Carleton College: Northfield, MN, 1984.

Table I. Visible-UV Spectra of Ruthenium(II) Complexes in Acetonitrile^a

compd	$d\pi \rightarrow \pi_1^*$	$d\pi \rightarrow \pi_2^*$	$\pi \rightarrow \pi^*$
[Ru(bpz) ₂ (bpm)] ²⁺	450 (1.5 × 10 ⁴), 420 (sh)	340 (sh)	295 (5.1 × 10 ⁴), 260 (3.7 × 10 ⁴)
[Ru(bpm) ₂ (bpz)] ²⁺	454 (9.6 × 10 ³), 430 (sh)	340 (sh)	300 (2.1 × 10 ⁴), 257 (3.5 × 10 ⁴)
[Ru(bpz)(bpm)(bpy)] ²⁺	464 (1.0 × 10 ⁴), 453 (sh), 430 (sh)	385 (sh)	295 (sh), 283 (3.6 × 10 ⁴), 266 (3.4 × 10 ⁴)
[Ru(bpy) ₂ ((CH ₃) ₂ bpy)] ²⁺	454 (2.0 × 10 ⁴)	359 (8.6 × 10 ³)	329 (1.4 × 10 ⁴), 290 (1.0 × 10 ⁵), 248 (3.5 × 10 ⁴)
[Ru((CH ₃) ₂ bpy) ₂ (bpy)] ²⁺	456 (1.3 × 10 ⁴)	359 (7.2 × 10 ³)	324 (1.1 × 10 ⁴), 288 (6.2 × 10 ⁴), 249 (2.2 × 10 ⁴)
[Ru(bpy) ₂ (py) ₂] ²⁺	457 (7.7 × 10 ³)	339 (1.2 × 10 ⁴)	291 (4.2 × 10 ⁴), 246 (2.2 × 10 ⁴)
[Ru((CH ₃) ₂ bpy) ₂ (py) ₂] ²⁺	439 (8.7 × 10 ³)	339 (1.2 × 10 ⁴)	285 (5.0 × 10 ⁴), 247 (2.1 × 10 ⁴)
[Ru(bpm) ₂ (py) ₂] ²⁺	471 (5.7 × 10 ³)	342 (1.4 × 10 ⁴)	267 (3.1 × 10 ⁴), 243 (3.7 × 10 ⁴)
[Ru(bpz) ₂ (py) ₂] ²⁺	472 (1.1 × 10 ⁴)	303 (4.3 × 10 ⁴)	240 (2.3 × 10 ⁴)
[Ru(bpz)(bpy)(py) ₂] ²⁺	484 (8.9 × 10 ³), 412 (7.4 × 10 ³)		292 (4.7 × 10 ⁴), 240 (3.6 × 10 ⁴)
[Ru(bpm) ₂ (CH ₃ CN)Cl] ^{+b}	487 (5.8 × 10 ³)	369 (1.1 × 10 ⁴)	258 (2.8 × 10 ⁴), 239 (3.7 × 10 ⁴)
[Ru(bpz) ₂ (CH ₃ CN)Cl] ^{+b}	492 (9.0 × 10 ³)	361 (7.1 × 10 ³)	305 (3.9 × 10 ⁴), 240 (2.1 × 10 ⁴)
[Ru(bpm) ₂ Cl ₂] ^c	571 (5.0 × 10 ³), 525 (5.1 × 10 ³)	415 (8.3 × 10 ³)	263 (sh), 243 (2.9 × 10 ⁴)
[Ru(bpz) ₂ Cl ₂] ^c	562 (9.2 × 10 ³)	400 (7.4 × 10 ³)	313 (2.8 × 10 ⁴), 244 (1.8 × 10 ⁴)
[Ru(bpy) ₃] ^{2+d}	451 (1.4 × 10 ⁴)	345 (6.5 × 10 ³), 323 (6.5 × 10 ³)	285 (8.7 × 10 ⁴), 250 (2.5 × 10 ⁴), 238 (3.0 × 10 ⁴)
[Ru(bpm) ₃] ²⁺	454 (8.6 × 10 ³), 418 (8.2 × 10 ³)	362 (sh), 332 (1.7 × 10 ⁴)	252 (4.9 × 10 ⁴)
[Ru(bpz) ₃] ^{2+d}	440 (1.3 × 10 ⁴), 415 (sh)	338 (sh)	291 (5.1 × 10 ⁴), 240 (2.0 × 10 ⁴)

^a λ_{\max} in nm, ± 1 nm; ϵ in parentheses, M⁻¹ cm⁻¹; 25 \pm 1 °C. ^b Values similar to those in ref 15. ^c From ref 15. ^d From ref 14a.

The reaction of [Ru(bpm)₂(CH₃CN)Cl]⁺ in neat pyridine resulted in formation of [Ru(bpm)₂(py)Cl]⁺. This formation was verified by an elemental analysis of the PF₆⁻ salt. Rather than those of Scheme I, the synthetic routes in Scheme II were found effective for the preparation of the bis(pyridine) complexes.

According to Scheme II, two approaches were used to prepare an ill-defined intermediate formulated as [Ru(L-L)₂(TRIF)₂]-TRIF·xHTRIF, where L-L = bpy, (CH₃)₂bpy, bpm, or bpz, TRIF is the triflate anion (CF₃SO₃⁻), and HTRIF is triflic acid (HC-F₃SO₃). The first approach involved refluxing the appropriate tris chelate complex in neat triflic acid. [Ru(bpy)₃](TRIF)₂, for example, underwent the following color changes upon reflux. The initial orange color changed to the characteristic green of [Ru(bpy)₃]³⁺ and finally blue. Isolation of the blue species and its subsequent reactions in acetonitrile and pyridine led to [Ru(bpy)₂(CH₃CN)₂]²⁺ and [Ru(bpy)₂(py)₂]²⁺, respectively. To effect formation of a similar triflate intermediate for the bipyrimidine analogue, it was necessary to use a second approach. In this case, the [Ru(bpm)₂(CH₃CN)Cl]⁺ complex was added to neat triflic acid and the solution was refluxed. Cl⁻ was removed as HCl(g), and CH₃CN was displaced by the large excess of HTRIF. On the basis of elemental analyses, color changes that indicate a higher valent ruthenium species is generated in HTRIF, and the subsequent chemistry leading to bis(pyridine) complexes, the intermediate is formulated as a ruthenium(III) species with two triflate ions coordinated as ligands.

Visible-UV Properties. A summary of the important visible-ultraviolet features is given in Table I. The absorptions are listed as $d\pi \rightarrow \pi_1^*$, $d\pi \rightarrow \pi_2^*$, and $\pi \rightarrow \pi^*$ transitions. The $\pi \rightarrow \pi^*$ transitions of ruthenium heterocyclic ligand complexes are generally observed in the 240–290-nm region.^{23,24} The π^* levels of the bpy, bpm, and bpz ligands are at different energies, as indicated by their reduction potentials above. Thus, mixed-ligand complexes are expected to give rise to more than one $d\pi \rightarrow \pi^*$ and $\pi \rightarrow \pi^*$ transition. In [Ru(bpy)₃]²⁺ itself, a series of transitions are expected to occur.²³ The first of these series is assigned as $d\pi \rightarrow \pi_1^*$; the second, approximately 6000 cm⁻¹ above the first, is assigned as $d\pi \rightarrow \pi_2^*$. In mixed-ligand complexes, the lowest energy absorption can be assigned to the ligand having the lowest energy π^* level. This is consistent with the lowest energy transition assigned as $d\pi \rightarrow \pi_1^*$ (bpz), the intermediate one as $d\pi \rightarrow \pi_1^*$ (bpm), and the highest energy one as $d\pi \rightarrow \pi_1^*$ (bpy). For [Ru(bpz)(bpm)(bpy)]²⁺ there are three such $d\pi \rightarrow \pi_1^*$ transitions.

Table II. Polarographic Half-Wave Potentials for Ruthenium(II) Complexes^{a,b}

compd	oxidn $E_{1/2}$	redn			$\Delta E_{1/2}$
		$E_{1/2}(1)$	$E_{1/2}(2)$	$E_{1/2}(3)$	
[Ru(bpz) ₂ (bpm)] ²⁺	1.87	-0.75	-0.95	-1.20	2.62
[Ru(bpm) ₂ (bpz)] ²⁺	1.78	-0.79	-1.04	-1.24	2.57
[Ru(bpz)(bpm)(bpy)] ²⁺	1.66	-0.83	-1.10	-1.24	2.49
[Ru(bpz)(bpy)(py) ₂] ²⁺	1.56	-0.88	-1.47		2.44
[Ru(bpy) ₂ (py) ₂] ²⁺	1.27	-1.35	-1.57		2.62
[Ru((CH ₃) ₂ bpy) ₂ (py) ₂] ²⁺	1.20	-1.46	-1.65		2.66
[Ru((CH ₃) ₂ bpy) ₃] ²⁺	1.12	-1.45	-1.63		2.57
[Ru((CH ₃) ₂ bpy) ₂ (bpy)] ²⁺	1.18	-1.43	-1.64	-1.87	2.61
[Ru(bpm) ₂ (py) ₂] ²⁺	1.49	-1.03	-1.21		2.52
[Ru(bpy) ₂ ((CH ₃) ₂ bpy)] ²⁺	1.24	-1.36	-1.56	-1.82	2.60
[Ru(bpz) ₂ (py) ₂] ²⁺	1.76	-0.77	-1.00		2.53
[Ru(bpm) ₂ (CH ₃ CN)Cl] ⁺	1.15	-1.09	-1.24		2.24
[Ru(bpz) ₂ (CH ₃ CN)Cl] ⁺	1.37	-0.92	-1.17		2.29
[Ru(bpm) ₂ Cl ₂] ^c	0.58	-1.28	-1.51		1.86
[Ru(bpz) ₂ Cl ₂] ^c	0.82	-1.09	-1.22		1.91
[Ru(bpy) ₃] ²⁺	1.27	-1.31	-1.50	-1.77	2.58
[Ru(bpm) ₃] ^{2+d}	1.69	-0.91	-1.08	-1.28	2.60
[Ru(bpz) ₃] ^{2+d}	1.98	-0.68	-0.87	-1.14	2.66
[Ru(bpy) ₂ (bpz)] ^{2+d}	1.49	-0.91	-1.45	-1.68	2.40
[Ru(bpy) ₂ (bpm)] ^{2+d}	1.40	-1.02	-1.45		2.42
[Ru(bpz) ₂ (bpy)] ^{2+d}	1.72	-0.79	-1.02	-1.58	2.51
[Ru(bpm) ₂ (bpy)] ²⁺	1.55	-0.95	-1.13		2.50

^a Potentials are in V vs SSCE. ^b Solutions were 0.10 M in TBAH; the solvent was acetonitrile; $T = 25 \pm 1$ °C. ^c The results are in general agreement with ref 15, but the positions of the waves are shifted somewhat. ^d From ref 14a.

The higher energy $d\pi \rightarrow \pi_2^*$ and $\pi \rightarrow \pi^*$ transitions for the complexes overlap appreciably and are difficult to assign to a specific ligand.

The low-energy transition shifted to the red as the number of chloride ligands increased. A similar red shift was observed for [Ru(bpy)₂XY]²⁺ where X is pyrazine and Y is chloride.²⁵ The shift can be rationalized on the basis of reduction in symmetry and σ -donor or π -withdrawal properties of the X and Y ligands.

Electrochemistry. $E_{1/2}$ values were determined from cyclic voltammograms and are summarized in Table II. For most redox couples, the anodic to cathodic current ratio was 1 and the difference between the cathodic and anodic peak positions of a given redox couple, ΔE_p , varied from 60 to 70 mV, indicative of a reversible, one-electron-transfer process.²⁶ The exception to this was the second reduction of the acetonitrile chloro complexes.

(23) Rillema, D. P.; Callahan, R. W.; Mack, K. B. *Inorg. Chem.* **1982**, *21*, 2589.

(24) (a) Felix, F.; Ferguson, J.; Gudel, H. U.; Ludi, A. *J. Am. Chem. Soc.* **1980**, *102*, 4086. (b) Descurtius, S.; Felix, F.; Ferguson, J.; Gudel, H. U.; Ludi, A. *Ibid.* **1980**, *102*, 4102.

(25) (a) Callahan, R. W.; Brown, G. M.; Meyer, T. J. *Inorg. Chem.* **1975**, *14*, 1443. (b) Powers, M. J.; Meyer, T. J. *Ibid.* **1978**, *17*, 2955.

(26) Nicholson, R. S.; Shain, I. *Anal. Chem.* **1964**, *36*, 705.

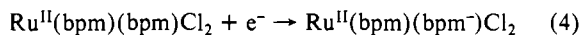
Table III. Luminescence Quantum Yields, Excited-State Lifetimes, and Quantum Yields for Ru(II) Complexes^a

compd	λ_{\max} , nm ^b	τ_0 , ns	ϕ_r^c	ϕ_p^d	ϕ_i^e	ϕ_{d-d}^f	ligand lost
[Ru(bpz) ₂ (bpm)] ²⁺	633 ^g	1053	0.041	0.24	0.53	0.45	bpz
[Ru(bpm) ₂ (bpz)] ²⁺	655 ^g	338 ^{g,h}	0.032	0.091	0.10	0.91	bpz
[Ru(bpz)(bpm)(bpy)] ²⁺	684 ^g	823	0.016	0.00038	0.25	0.0015	bpz
[Ru(bpy) ₂ (py) ₂] ²⁺	610		0.00086	0.0059			py
[Ru((CH ₃) ₂ bpy) ₂ (py) ₂] ²⁺	615		0.00018	0.025			py
[Ru((CH ₃) ₂ bpy) ₃] ²⁺	625	777	0.041	0.0044	0.33	0.013	(CH ₃) ₂ bpy
[Ru((CH ₃) ₂ bpy) ₂ (bpy)] ²⁺	646	984	0.035	0.0041			
[Ru(bpm) ₂ (py) ₂] ²⁺	665		0.0018	0.048			py
[Ru(bpy) ₂ ((CH ₃) ₂ bpy)] ²⁺	640	1066	0.040	0.0026			
[Ru(bpz) ₂ (py) ₂] ²⁺	665	570	0.0156	0.070	0.56	0.13	py
[Ru(bpz)(bpy)(py) ₂] ²⁺	684		0.0057	0.00088			py
[Ru(bpy) ₂ (bpz)] ²⁺	710 ^g	376 ^{g,h}	0.0056	0.00017	0.02	0.0085	bpz
[Ru(bpy) ₂ (bpm)] ²⁺	710 ^g	76 ^{g,h}	0.0011	0.0003	0.11	0.0027	bpm
[Ru(bpm) ₂ (bpy)] ²⁺	670 ^g	182 ^{g,h}	0.0038	0.0016	0.06	0.027	bpm
[Ru(bpz) ₂ (bpy)] ²⁺	654 ^{g,h}	1099 ^{g,h}	0.040	0.0049	0.17	0.029	bpz
[Ru(bpm) ₂ (CH ₃ CN)Cl] ⁺	788	<7	0.000018	0.0007			CH ₃ CN
[Ru(bpz) ₂ (CH ₃ CN)Cl] ⁺	766	56	0.00018	0.0052			CH ₃ CN
[Ru(bpy) ₃] ²⁺	620 ^g	800 ^{g,h}	0.042	0.0021	0.46	0.0046	bpy
[Ru(bpm) ₃] ²⁺	639 ^g	131 ^{g,h}	0.0028	0.043	0.70	0.061	bpm
[Ru(bpz) ₃] ²⁺	610 ^g	795 ^{g,h}	0.034	0.35	0.68	0.51	bpz

^a In acetonitrile unless otherwise noted; $T = 25 \pm 1$ °C. ^b $\lambda_{\max} = 436 \pm 1$ nm; λ_{\max} corrected. ^c Radiative quantum yield, $\pm 5\%$; $\lambda_{\text{ex}} = 436$ nm. ^d Photochemical quantum yield, $\pm 5\%$; $\lambda_{\text{ex}} = 436$ nm; 1 mM (TEA)Cl. ^e Intersystem crossing quantum yield from the ³MLCT to the d-d state. ^f Fraction of photosubstitution. ^g In propylene carbonate. ^h Data from ref 8 and: Allen, G. M.S. Thesis, The University of North Carolina.

Here, the second reduction was quasi-reversible with ΔE_p values on the order of 90–100 mV. Both Ru(bpm)₂Cl₂ and [Ru(bpm)₂(CH₃CN)Cl]⁺ were unstable at $E_{1/2}$ values more negative than -1.0 V vs SSCE. The instability was noted by the appearance of a stripping wave upon the reoxidation cycle.

Figure 3 illustrates the trend observed between the potentials for the first oxidation and the first reduction of the ruthenium complexes containing bpm and bpz ligands. The first oxidation is associated with removal of an electron from the metal center (eq 3); the first reduction is associated with addition of an electron to one of the heterocyclic ligands (eq 4). In mixed-ligand com-



plexes, the first reduction is associated with the reduction of the ligand with the lowest π^* energy level,^{8b} which, for the compounds in Table II, is the bpz ligand, then the bpm ligand, and finally the bpy ligand. The redox potentials for the first oxidation and first reduction of the ruthenium complexes become more positive in the sequence dichloro → acetonitrile chloro → tris. The shift can be rationalized on the basis of the ligand field strengths, which vary in the order bpz > CH₃CN > Cl. The difference in positive change given by the slope of 2.5 in Figure 3 indicates that the effect on the potential of the first reduction is less marked than on the potential of the first oxidation. This means the d π levels change energy more rapidly than the π^* levels as the ligands about ruthenium(II) are varied. This is reasonable, given that the primary effect of altering these energy levels will be related to the ligand field strength followed by the secondary effect of π bonding between the metal d π and ligand π^* orbitals.

The three reduction potentials for each tris ruthenium complex in Table II are associated with the stepwise reduction of each heterocyclic ligand.²⁷ For mixed-ligand complexes, the expected order from the least negative to the most negative potentials is bpz > bpm > bpy. Each of the ligands is reduced once, prior to double reduction. This assessment is based on analogy to the redox potentials of the parent tris chelates given in Table II.

Emission and Photosubstitution Properties. Optical excitation by visible or ultraviolet light gives rise to luminescence at room temperature for most of the compounds except for Ru(bpm)₂Cl₂ and Ru(bpz)₂Cl₂, which are nonluminescing in the spectral range of the instrumentation (200–850 nm). Corrected spectral emission

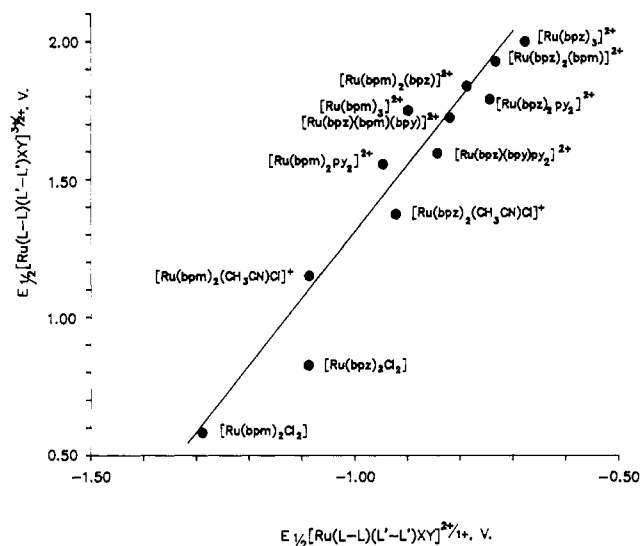


Figure 3. Correlation between the redox potential for oxidation, Ru(III/II), and for reduction, Ru(II/I). The slope is 2.5, and the correlation coefficient is 0.97.

maxima are given in Table III and compared to the parent tris and analogous bpy compounds. Starting with [Ru(bpz)₃]²⁺, luminescence maxima red-shift and energy maxima follow the order [Ru(bpz)₃]²⁺ > [Ru(bpz)₂(L-L)]²⁺ > [Ru(bpz)(L-L)₂]²⁺ > [Ru(bpz)(bpm)(bpy)]²⁺ > [Ru(bpy)₂(CH₃CN)Cl]⁺, where L-L is bpm, bpy, or (py)₂. In like manner, starting with [Ru(bpy)₃]²⁺, the energy order is [Ru(bpy)₃]²⁺ > [Ru(bpy)(L-L)₂]²⁺, [Ru(bpz)(bpm)(bpy)]²⁺ > [Ru(bpy)(L-L)₂]²⁺, where L-L is bpm, bpz, or (py)₂.

Excited-state lifetimes determined at room temperature ranged from 1099 ns for [Ru(bpz)₂(bpy)]²⁺ to <7 ns for [Ru(bpm)₂(CH₃CN)Cl]⁺, and radiative quantum yields ranged from 0.042 for [Ru(bpy)₃]²⁺ to 1.8×10^{-5} for [Ru(bpm)₂(CH₃CN)Cl]⁺. The radiative quantum yields of [Ru(bpz)₂(bpy)]²⁺ and [Ru(bpz)₂(bpm)]²⁺ compare favorably to the one for [Ru(bpy)₃]²⁺, although the lifetimes differ somewhat.

Ligand loss quantum yields were determined for all of the compounds in Table III. Photosubstitution was studied in acetonitrile in the presence of 1 mM Cl⁻. Two classes of compounds were studied, those with the bidentate ligands and those with two bidentate and two monodentate ligands, and their photosubstitution is illustrated in eq 1. The final products were the acetonitrile chloro

(27) Kober, E. M.; Marshall, J. L.; Dressick, W. J.; Sullivan, B. P.; Caspar, J. V.; Meyer, T. J. *Inorg. Chem.* **1985**, *24*, 2755.

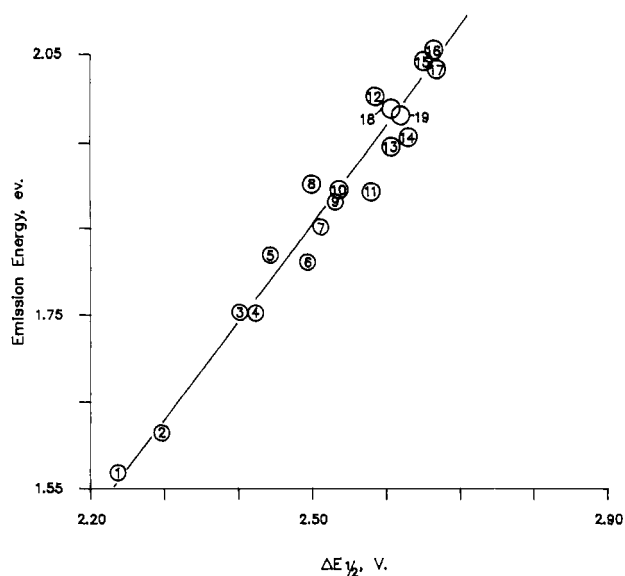


Figure 4. Relationship between the emission energy maxima and the energy gap as given by $\Delta E_{1/2}$, where $\Delta E_{1/2} = E_{1/2}(\text{Ru(III/II)}) - E_{1/2}(\text{Ru(II/I)})$. The slope is 1.1, the intercept is -0.88 , and the correlation coefficient is 0.98. Numbers and corresponding compounds are as follows: 1, $[\text{Ru}(\text{bpm})_2(\text{CH}_3\text{CN})\text{Cl}]^+$; 2, $[\text{Ru}(\text{bpz})_2(\text{CH}_3\text{CN})\text{Cl}]^+$; 3, $[\text{Ru}(\text{bpy})_2(\text{bpz})]^{2+}$; 4, $[\text{Ru}(\text{bpy})_2(\text{bpm})]^{2+}$; 5, $[\text{Ru}(\text{bpz})_2(\text{bpy})(\text{py})_2]^{2+}$; 6, $[\text{Ru}(\text{bpz})_2(\text{bpm})(\text{bpy})]^{2+}$; 7, $[\text{Ru}(\text{bpz})_2(\text{bpy})]^{2+}$; 8, $[\text{Ru}(\text{bpm})_2(\text{bpy})]^{2+}$; 9, $[\text{Ru}(\text{bpz})_2(\text{py})_2]^{2+}$; 10, $[\text{Ru}(\text{bpm})_2(\text{py})_2]^{2+}$; 11, $[\text{Ru}(\text{bpm})_2(\text{bpz})]^{2+}$; 12, $[\text{Ru}(\text{bpy})_3]^{2+}$; 13, $[\text{Ru}(\text{bpm})_3]^{2+}$; 14, $[\text{Ru}(\text{bpz})_2(\text{bpm})]^{2+}$; 15, $[\text{Ru}(\text{bpy})_2(\text{py})_2]^{2+}$; 16, $[\text{Ru}((\text{CH}_3)_2\text{bpy})_2(\text{py})_2]^{2+}$; 17, $[\text{Ru}(\text{bpz})_3]^{2+}$; 18, $[\text{Ru}(\text{bpy})_2((\text{CH}_3)_2\text{bpy})]^{2+}$; 19, $[\text{Ru}((\text{CH}_3)_2\text{bpy})_2(\text{bpy})]^{2+}$.

or pyridine chloro derivative in the first reaction and the dichloro analogue in the second reaction. The geometry of the products remained cis. The compounds studied for the second chloride ligand substitution were independently synthesized and purified prior to the photolysis study. Equivalent thermal reactions did not proceed to a measurable degree within the time frame of the experiments, and O_2 was removed from the solutions to avoid the possibility of quenching effects or side reactions. The quantum yields for the second step were 2–3 orders of magnitude smaller than those of the first step. Hence, photosubstitution in the first step could be studied with only a negligible contribution due to secondary photolysis.

The dominant reaction pathway for the mixed-ligand tris chelates was loss of the bidentate ligand with the lowest π^* energy level. This was clear on the basis of the chemistry given in Scheme 1 and the specific reaction sequences required to lead to formation of $[\text{Ru}(\text{bpy})(\text{bpm})(\text{bpz})]^{2+}$.

Product identification was also carried out for photosubstitution of bis(pyridine) complexes. Two methods were used in this determination, product analysis following exhaustive photolysis and an NMR investigation during photolysis. The product analysis experiment involved bulk photolysis of 0.144 mM $[\text{Ru}(\text{bpm})_2(\text{py})_2](\text{TRIF})_2$ in acetonitrile containing 0.144 mM $(\text{TEA})\text{Cl}$. The product $[\text{Ru}(\text{bpm})_2(\text{py})\text{Cl}](\text{TRIF})$ was collected, and the following elemental analysis was obtained. Found: C, 38.79; N, 18.51; H, 2.51; Cl, 5.20. Calcd: C, 38.66; N, 18.46; H, 2.58; Cl, 5.14.

The NMR experiment consisted of studying the photosubstitution of $[\text{Ru}(\text{bpz})_2(\text{py})_2]^{2+}$ with Cl^- (1:1) in deuterated acetonitrile. The ratios of a proton resonance peak associated with coordinated bipyrazine to a proton resonance peak belonging to coordinated pyridine increased from 1.00 to 1.14 upon 8.9% photolysis to 1.49 upon 15.5% photolysis. This indicated that the number of coordinated pyridine ligands decreased during photolysis. The free pyridine ligand was not detected because of the much higher concentration of the ruthenium complex compared to the concentration of the free pyridine in solution.

Discussion

Energy Gap Correlations. Correlations were found between the energy gap expressed by $\Delta E_{1/2}$, where $\Delta E_{1/2}$ is the positive po-

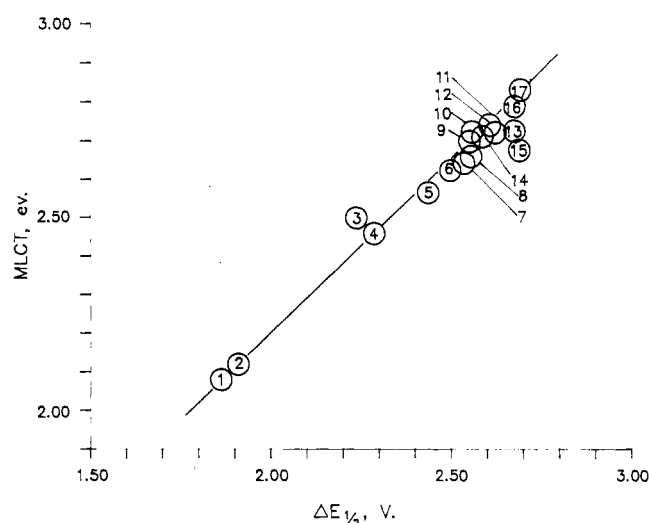
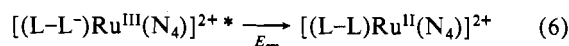
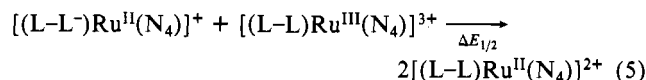


Figure 5. Relationship between the $^1\text{MLCT}$ energy maxima and the energy gap as given by the difference in redox potentials between the Ru(III/II) couple and the Ru(II/I) couple. The slope is 0.75, the intercept is 0.77, and the correlation coefficient is 0.99. Numbers and corresponding compounds are as follows: 1, $[\text{Ru}(\text{bpm})_2\text{Cl}_2]$; 2, $[\text{Ru}(\text{bpz})_2\text{Cl}_2]$; 3, $[\text{Ru}(\text{bpm})_2(\text{CH}_3\text{CN})\text{Cl}]^+$; 4, $[\text{Ru}(\text{bpz})_2(\text{CH}_3\text{CN})\text{Cl}]^+$; 5, $[\text{Ru}(\text{bpz})_2(\text{bpy})(\text{py})_2]^{2+}$; 6, $[\text{Ru}(\text{bpz})_2(\text{bpm})(\text{bpy})]^{2+}$; 7, $[\text{Ru}(\text{bpm})_2(\text{py})_2]^{2+}$; 8, $[\text{Ru}(\text{bpz})_2(\text{py})_2]^{2+}$; 9, $[\text{Ru}(\text{bpm})_2(\text{bpz})]^{2+}$; 10, $[\text{Ru}(\text{bpy})_3]^{2+}$; 11, $[\text{Ru}(\text{bpz})_2(\text{bpm})]^{2+}$; 12, $[\text{Ru}(\text{bpy})_2((\text{CH}_3)_2\text{bpy})]^{2+}$; 13, $[\text{Ru}((\text{CH}_3)_2\text{bpy})_2(\text{bpy})]^{2+}$; 14, $[\text{Ru}(\text{bpm})_3]^{2+}$; 15, $[\text{Ru}(\text{bpy})_2(\text{py})_2]^{2+}$; 16, $[\text{Ru}(\text{bpz})_3]^{2+}$; 17, $[\text{Ru}(\text{CH}_3)_2\text{bpy})_2(\text{py})_2]^{2+}$.

tential difference between the first oxidation and the first reduction, and the $^1\text{MLCT}$ absorption energy maxima (E_{MLCT}), the corrected emission energy maxima (E_{em}), and the photochemical quantum yield (ϕ_p). The spectroscopic correlation between E_{em} and $\Delta E_{1/2}$ is expected. The $\Delta E_{1/2}$ parameter is the outer-sphere analogue²⁷ of the intramolecule emission process as shown in eq 5 and 6. The



correlation is shown in Figure 4; the slope is 1.1, the correlation coefficient is 0.98, and the intercept is -0.88 . The nonzero intercept contains components related to the electrostatic character of the $d\pi^5\pi^*$ electronic configuration and vibrational components related to $E_{0,0}$, the energy difference between the zeroth vibrational level of the excited $^3\text{MLCT}$ state and the zeroth vibrational level of the ground state. The slope, however, is near unity and noteworthy in showing that the same features of the $d\pi$ and π^* orbitals of the ground states are carried over to the excited state.

In the past, the red shift of E_{em} in concert with the $^1\text{MLCT}$ absorption energy has been noted.^{14,28} A plot of E_{MLCT} (in eV) vs E_{em} (in eV) for the compounds studied here was linear with a correlation coefficient of 0.97. The slope was 0.6, and the intercept was 1.6 eV. This observation suggested that a correlation between E_{MLCT} and $\Delta E_{1/2}$ should also be linear. Indeed, as shown in Figure 5, the plot is linear with a slope of 0.77, a correlation coefficient of 0.99, and an intercept of 0.74. The correlation includes a wide range of compounds and illustrates the close relationship that exists between excited-state and ground-state properties of ruthenium(II) heterocycles. A correlation of this type was previously reported by Lever and Dodsworth²⁹ for $[\text{Ru}(\text{bpy})_2\text{XY}]^{n+}$ complexes where X and Y were various ligands and more recently by Barigelletti and co-workers³⁰ for ruthenium heterocyclic ligand complexes.

(28) Fuchs, Y.; Lofters, S.; Dieter, T.; Shi, W.; Morgan, R.; Streaks, T. C.; Gafney, H. D.; Baker, A. D. *J. Am. Chem. Soc.* **1987**, *109*, 2691.

(29) Dodsworth, E. S.; Lever, A. B. P. *Chem. Phys. Lett.* **1986**, *124*, 152.

(30) Barigelletti, F.; Juris, A.; Balzani, V.; Belsler, P.; von Zelewsky, A. *Inorg. Chem.* **1987**, *26*, 4115.

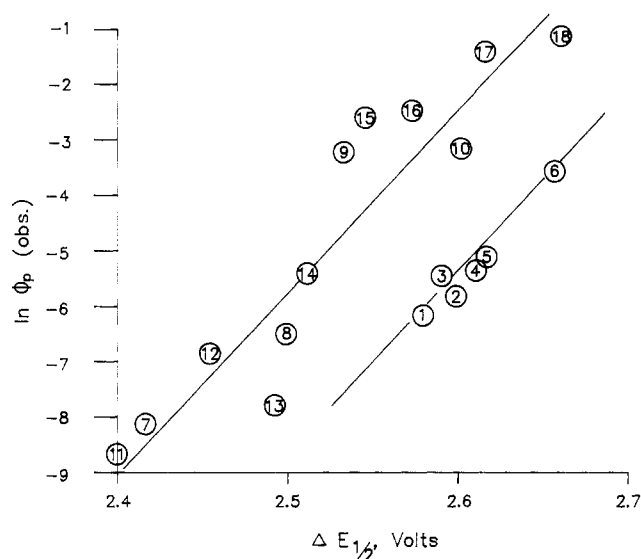


Figure 6. Correlation between the photochemical substitution quantum yield and the energy gap $\Delta E_{1/2}$. The slope is 32, the intercept is -87 , and the correlation is 0.96. Numbers and corresponding compounds are as follows. bpy series: 1, $[\text{Ru}(\text{bpy})_3]^{2+}$; 2, $[\text{Ru}(\text{bpy})_2(\text{CH}_3)_2\text{bpy}]^{2+}$; 3, $[\text{Ru}((\text{CH}_3)_2\text{bpy})_3]^{2+}$; 4, $[\text{Ru}((\text{CH}_3)_2\text{bpy})_2(\text{bpy})]^{2+}$; 5, $[\text{Ru}(\text{bpy})_2(\text{py})_2]^{2+}$; 6, $[\text{Ru}((\text{CH}_3)_2\text{bpy})_2(\text{py})_2]^{2+}$. bpm series: 7, $[\text{Ru}(\text{bpy})_2(\text{bpm})]^{2+}$; 8, $[\text{Ru}(\text{bpm})_2(\text{bpy})]^{2+}$; 9, $[\text{Ru}(\text{bpm})_2(\text{py})_2]^{2+}$; 10, $[\text{Ru}(\text{bpm})_3]^{2+}$. bpz series: 11, $[\text{Ru}(\text{bpy})_2(\text{bpz})]^{2+}$; 12, $[\text{Ru}(\text{bpz})(\text{bpy})(\text{py})_2]^{2+}$; 13, $[\text{Ru}(\text{bpz})(\text{bpm})(\text{bpy})]^{2+}$; 14, $[\text{Ru}(\text{bpz})_2(\text{bpy})]^{2+}$; 15, $[\text{Ru}(\text{bpz})_2(\text{py})_2]^{2+}$; 16, $[\text{Ru}(\text{bpm})_2(\text{bpz})]^{2+}$; 17, $[\text{Ru}(\text{bpz})_2(\text{bpm})]^{2+}$; 18, $[\text{Ru}(\text{bpz})_3]^{2+}$.

One of the more revealing correlations is shown in Figure 6. The log of the observed photochemical quantum yield for the closely related ligand systems is a linear function of the energy gap as expressed by $\Delta E_{1/2}$. Two linear correlations are observed. The correlation coefficient for the bpm–bpz series is 0.96; that of the bpy series is 0.97. The linear relationships imply that photochemistry for bpy, bpm, and bpz complexes is controlled by the energy gap. The justification for this can be related to the energy gap law, which previously has been shown to linearly correlate $-\ln k_{nr}$ with E_{em} .⁸ Further, the linear relationship between E_{em} and $\Delta E_{1/2}$ has been illustrated here and previously.^{27,31}

Application of the approach of ref 3b and ref 32 to the photochemical processes in Figure 1 leads to eq 7, which defines the

$$\phi_p = \eta_{isc} \left(\frac{k_a}{k_r + k_{nr} + k_a} \right) \left(\frac{k_p}{k_p + k'_{nr} + k_b} \right) \quad (7)$$

photosubstitution quantum yield in terms of photophysical properties. In eq 7, η_{isc} is the intersystem-crossing quantum yield from the $^1\text{MLCT}$ state to the $^3\text{MLCT}$ state, k_r is the radiative decay rate constant from the $^3\text{MLCT}$ state to ^1GS , k_{nr} is the nonradiative rate constant from the $^3\text{MLCT}$ state to ^1GS , k_a is the rate constant for electron transfer from the $^3\text{MLCT}$ state to the ligand field state, k_p is the photochemical rate constant from the ligand field state, k'_{nr} is the nonradiative rate constant from the ligand field state to ^1GS , and k_b is the rate constant for back electron transfer from the ligand field state to the $^3\text{MLCT}$ state. The constant k_p is really $K_{IP}k_s$, where K_{IP} is the ion-pairing constant and k_s is the photosubstitution rate constant. Substitutions were studied in the concentration range ($8 \times 10^{-4} \text{ M} < [\text{Cl}^-] < 4 \times 10^{-3} \text{ M}$); hence, k_p was independent of the Cl^- concentration.³³ According to eq 7, then, the quantum yield ϕ_p depends on the fraction of energy transferred to the $^3\text{MLCT}$ state, the fraction that crosses over into the excited ligand field manifold

(d–d state), and the fraction of energy that results in photosubstitution from the d–d state.

Equation 7 can be simplified. The intersystem-crossing quantum yield from the $^1\text{MLCT}$ state to the $^3\text{MLCT}$ state for $[\text{Ru}(\text{bpy})_3]^{2+}$ is known to be 1 over a wide range of wavelengths^{34,35} and in our previously published work with mixed-ligand complexes of ruthenium(II) containing bpy, bpm, bpz, and bpq, where bpq is 2,3-bis(2-pyridyl)quinoxaline (shown in Figure 1), was also assumed to be 1.⁸ This assumption was reasonable, given the similarity of the complexes. Equation 7 can be rewritten as eq 8.

$$\phi_p \approx \left(\frac{k_a}{k_r + k_{nr} + k_a} \right) \left(\frac{k_p}{k_p + k'_{nr} + k_b} \right) \quad (8)$$

There are several limits that give rise to a linear $\ln \phi_p$ energy gap law dependence.

(1) Under conditions where $k_{nr} > (k_r + k_a)$, eq 8 reduces to eq 9, which expressed in logarithm form gives eq 10. The pro-

$$\phi_p \approx \frac{1}{k_{nr}} \left(\frac{k_a k_p}{k_p + k'_{nr} + k_b} \right) \quad (9)$$

$$\ln \phi_p \approx -\ln k_{nr} + \ln \left(\frac{k_a k_p}{k_p + k'_{nr} + k_b} \right) \quad (10)$$

portionality between $\ln \phi_p$ and $\Delta E_{1/2}$ then follows, provided the second log term remains relatively constant.

(2) For the condition $(k_{nr} + k_a) > k_r$, eq 8 reduces to eq 11.

$$\phi_p \approx \left(\frac{k_a}{k_{nr} + k_a} \right) \left(\frac{k_p}{k_p + k'_{nr} + k_b} \right) \quad (11)$$

This equation gives rise to a linear $\ln \phi_p$ dependence provided $k_a \sim k_{nr}$ or $k_a > k_{nr}$ and other reasonable limits are imposed. This is expressed in general terms in eq 12, which has the same form

$$\phi_p \approx \left(\frac{k_p}{k_p + k'_{nr} + k_b} \right) (\text{const}) \quad (12)$$

as presented in ref 32. For the limits $(k_p + k'_{nr}) > k_b$, decay of the ligand field state is rapid. Equation 12 reduces to eq 13,

$$\phi_p \approx \left(\frac{k_p}{k_p + k'_{nr}} \right) (\text{const}) \quad (13)$$

corresponding to the case of irreversible electron transfer from the $^3\text{MLCT}$ state to the d–d excited state. In most cases, ϕ_p values in Table III are less than 0.01, which means $k'_{nr} > k_p$ for complexes falling in the “irreversible” limit. The corresponding linear relationship is expressed in eq 14.

$$\ln \phi_p \approx -\ln k'_{nr} + \ln ((\text{const})k_p) \quad (14)$$

(3) For $k_b > (k_p + k'_{nr})$, the limits imposed in eq 9 will be met³⁶ and equilibrium is established between the ligand field state and the $^3\text{MLCT}$ state in which case eq 9 takes the form in eq 15, where

$$\phi_p \approx \left(\frac{1}{k_{nr}} \right) \left(\frac{k_a}{k_b k_p} \right) \approx \left(\frac{1}{k_{nr}} \right) K k_p \quad (15)$$

K represents the equilibrium described as $^3\text{MLCT} \rightleftharpoons \text{d–d state}$. Indeed, there is evidence that the electronically populated $^3\text{MLCT}$ state and the d–d state are in thermal equilibrium.³⁷ Again, the

(31) Juris, A.; Belsler, P.; Barigelletti, F.; von Zelewsky, A.; Balzani, V. *J. Phys. Chem.* **1987**, *91*, 1095.

(32) Barigelletti, F.; Juris, A.; Balzani, V.; Belsler, P.; von Zelewsky, A. *Inorg. Chem.* **1987**, *26*, 4115.

(33) The photochemical substitution quantum yield dependence on $[\text{Cl}^-]$ was studied for $[\text{Ru}(\text{bpy})_3]^{2+}$ in acetonitrile at 25 °C. The break point occurred at 0.8 mM.

(34) Demas, J. N.; Taylor, D. G. *Inorg. Chem.* **1979**, *18*, 3177.

(35) (a) Bensason, R.; Salet, C.; Balzani, V. *J. Phys. Chem.* **1976**, *80*, 2499. (b) Boletta, F.; Juris, A.; Mestri, M.; Sandrini, D. *Inorg. Chim. Acta* **1980**, *44*, L175.

(36) The constant k_{nr} is a factor of 10 or 100 times greater than k_p ,⁸ and linearity is retained in Figure 6. Therefore, at this time, eq 9 is the best approximation to the data.

linear relationship between $\ln \phi_p$ and $-\ln k_{nr}$ is obtained, provided the $\ln(Kk_p)$ term does not contribute significantly to the equation.

Thus, two equations relating ϕ_p to the energy gap are obtained: $\ln \phi_p \propto -\ln k_{nr}$ or $\ln \phi_p \propto -\ln k'_{nr}$, depending on the limits imposed.

The observed photochemical substitution quantum yields were normalized to values labeled ϕ_{d-d} , which give the fraction of photosubstitution events occurring from the d-d excited state ($\phi_{d-d} = \phi_p/\phi_i$), where ϕ_i is the quantum yield for crossing from the $^3\text{MLCT}$ state to the d-d excited state. ϕ_i values were calculated from activation parameters obtained from ref 8 in a fit of $1/\tau$ vs $1/T$. Complexes with $\phi_{d-d} > 0.1$ most likely have values that fall in the limit $(k_p + k'_{nr}) > k_b$. $[\text{Ru}(\text{bpy})_3]^{2+}$ is also thought³² to belong to the case with $(k_p + k'_{nr}) > k_b$, which probably means $k'_{nr} > k_b$ due to its low photochemical substitution quantum yield. Thus, complexes with fairly high activation energies, ΔE , from the $^3\text{MLCT}$ state to the d-d state can have different substitution quantum yields apparently due to the difference in the magnitude of k_p and k'_{nr} . Other complexes with low photosubstitution quantum yields, such as $[\text{Ru}(\text{bpy})_2(\text{bpz})]^{2+}$, most likely follow the other limit of $k_b > (k_p + k'_{nr})$. These complexes generally have low ΔE values. Mechanistic deactivation of the excited states for these complexes has also been attributed to a fourth state located just above the $^3\text{MLCT}$ state.⁸

The above discussion is predicted on intersystem crossing from the $^1\text{MLCT}$ state to the $^3\text{MLCT}$ state. There is some evidence for direct population of the d-d state from the $^1\text{MLCT}$ state.^{5,6} The evidence for this was derived from the temperature dependence of photoanation reactions. Photoanation of $[\text{Ru}(\text{bpy})_3]^{2+}$ was temperature dependent, whereas that of $[\text{Ru}(\text{bpy})_2(\text{py})_2]^{2+}$ was less temperature sensitive.^{3b} Hence, it was suggested that for $[\text{Ru}(\text{bpy})_2(\text{py})_2]^{2+}$ direct population of the d-d state from the $^1\text{MLCT}$ state was a possible explanation for the observed behavior. For complexes in Table III where this is true, ϕ_i values would be erroneous. However, it is important to note that $[\text{Ru}(\text{bpy})_3]^{2+}$ and $[\text{Ru}(\text{bpy})_2(\text{py})_2]^{2+}$ fall on the same line in Figure 6. Thus, the temperature dependence, while important, does not seem to alter the trends in Figure 6. This is encouraging, since photosubstitution behavior appears predictable within each series and appears less sensitive to the actual substitution mechanism.

In the past most of the emphasis on controlling photosubstitution in tris chelates of ruthenium(II) has focused on modifying the ligand field strength.^{4,8,28} The basic idea was to raise the energy of the d-d state such that it no longer would compete with the $^3\text{MLCT}$ state. Indeed, the idea has merit. Photosubstitution decreased in the order $[\text{Ru}(\text{bpz})_3]^{2+}$ ($\phi_p = 0.35$) $>$ $[\text{Ru}(\text{bpy})_2(\text{bpz})]^{2+}$ ($\phi_p = 1.7 \times 10^{-4}$) as the average ligand field strength increased [$pK_a(\text{pyridine}) = 5.2$;³⁸ $pK_a(\text{pyrazine}) = 0.8$ ³⁹]. The bpm and bpz complexes appear to form a special series as noted

in Figure 6. Other mixed-ligand complexes appear to form different classes. For example, $[\text{Ru}(\text{bpq})_3]^{2+}$, $[\text{Ru}(\text{bpq})_2(\text{bpy})]^{2+}$, and $[\text{Ru}(\text{bpy})_2(\text{bpq})]^{2+}$ form another series (not shown) that lies to the left of the bpm-bpz series. $[\text{Ru}(\text{bpy})_3]^{2+}$, $[\text{Ru}(\text{bpy})_2(\text{py})_2]^{2+}$, $[\text{Ru}((\text{CH}_3)_2\text{bpy})_2(\text{py})_2]^{2+}$, and $[\text{Ru}((\text{CH}_3)_2\text{bpy})_3]^{2+}$ form a series that lies to the right of the bpm-bpz series. These differences cannot be related to σ -donor strength only, since, according to the pK_a values, $\text{bpq} \approx \text{bpz} < \text{bpm} < \text{bpy}$ [$pK_a(\text{quinoxaline}) = 0.7$; $pK_a(\text{pyrimidine}) = 1.3$].⁴⁰ The location along the x axis in Figure 6 is more closely related to the energy of the free-ligand π^* orbitals as represented by their $E_{1/2}$ values for reduction (bpq, -1.56 V^{8b} ; bpz, -1.76 V^{15} ; bpm, -1.80 V^{19} ; bpy, -2.18 V^{20}).

While $\ln \phi_p(\text{obs})$ does correlate with $\Delta E_{1/2}$, the excited-state lifetime, τ , does not. Rather, for the series $[\text{Ru}(\text{L-L})_{3-n}(\text{bpy})_n]^{2+}$, $n = 0-3$, τ first increases and then decreases. Although k_{nr} and k_b may play a role, the results can probably be explained by the k_{nr} and k_a steps. As bpy is added, $\Delta E_{1/2}$ decreases but the d-d state increases in energy. The net result is k_{nr} and ΔE (Figure 1) increase. The increase in ΔE affects k_a , causing an increase in the excited-state lifetime. The opposing effects of both k_{nr} and ΔE then provide an explanation for the observed lifetime results and, for consistency, for the $\ln \phi_p(\text{obs})$ vs $\Delta E_{1/2}$ results.

In summary, the observed photochemical substitution quantum yields fall into various classes based on the ligand with the lowest π^* energy levels. Within each class, the higher the energy between the $^3\text{MLCT}$ and ^1GS , the more susceptible the complex is to photosubstitution. It would be misleading to imply that the ligand with the lowest energy π^* level is always lost in the photolysis. Rather, ligand loss is governed by bond strength in the excited state. Thus, monodentate ligands such as pyridine are lost in preference to bidentate chelates even though the π^* energy levels of pyridine are higher in energy than those of bipyrazine. Yet compounds such as $[\text{Ru}(\text{bpz})(\text{bpy})(\text{py})_2]^{2+}$ follow the trend in Figure 6 associated with bipyrazine compounds. It is interesting to note where $[\text{Ru}(\text{bpy})_3]^{2+}$ falls in photochemical stability among the various complexes listed in Table III. Only two other complexes, $[\text{Ru}(\text{bpy})(\text{bpm})(\text{bpz})]^{2+}$ and $[\text{Ru}(\text{bpy})_2(\text{bpm})]^{2+}$, have lower ϕ_{d-d} values.

Acknowledgment. We thank the Office of Basic Energy Sciences of the Department of Energy under Grant DE-FG05-84ER-13263 and the Foundation of the University of North Carolina at Charlotte for support. We also thank Johnson-Matthey, Inc., for supplying on loan the RuCl_3 used in these studies. H.B.R. thanks the Carolina Chemical Club for a fellowship during the 1985-86 academic year. We also thank Laura Worl for preliminary photophysical data on the bis(pyridine) complexes.

Supplementary Material Available: Table IV, listing elemental analyses for the compounds (1 page). Ordering information is given on any current masthead page.

(37) Ollino, M.; Cherry, W. R. *Inorg. Chem.* **1985**, *24*, 1417.

(38) *Handbook of Chemistry and Physics*, 42nd ed.; Chemical Rubber Co.: Cleveland, OH, 1960-61; p 1750.

(39) Ford, P.; Rudd, D. P.; Gaunder, R.; Taube, H. *J. Am. Chem. Soc.* **1968**, *90*, 1187.

(40) *Lange's Handbook of Chemistry*; 13th ed.; Dean, J. H., Ed.; McGraw-Hill: New York, 1985; sections 5.55, 5.56.